available at www.sciencedirect.com
journal homepage: www.europeanurology.com/eufocus

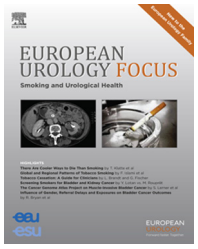

Platinum Priority – Review – Prostate Cancer
Editorial by XXX on pp. x–y of this issue

Rationale for Modernising Imaging in Advanced Prostate Cancer

Anwar R. Padhani[a,*], *Frederic E. Lecouvet*[b], *Nina Tunariu*[c], *Dow-Mu Koh*[c], *Frederik De Keyzer*[d], *David J. Collins*[c], *Evis Sala*[e], *Stefano Fanti*[f], *H. Alberto Vargas*[e], *Giuseppe Petralia*[g], *Heinz Peter Schlemmer*[h], *Bertrand Tombal*[i], *Johann de Bono*[j]

[a] *Paul Strickland Scanner Centre, Mount Vernon Hospital, Middlesex, UK;* [b] *Department of Radiology, Centre du Cancer and Institut de Recherche Expérimentale et Clinique, Cliniques Universitaires Saint-Luc, Université Catholique de Louvain, Brussels, Belgium;* [c] *Cancer Research UK Cancer Imaging Centre, Institute of Cancer Research and Royal Marsden NHS Foundation Trust, Surrey, UK;* [d] *Department of Radiology, Medical Imaging Research Centre, University Hospitals Leuven, Leuven, Belgium;* [e] *Department of Radiology, Memorial Sloan Kettering Cancer Center, New York, NY, USA;* [f] *Service of Nuclear Medicine, S.Orsola-Malpighi Hospital, University of Bologna, Bologna, Italy;* [g] *Department of Radiology, European Institute of Oncology, Milan, Italy;* [h] *Department of Radiology, German Cancer Research Center Heidelberg (DKFZ), Heidelberg, Germany;* [i] *Department of Urology, Cliniques Universitaires Saint-Luc, Université Catholique de Louvain, Brussels, Belgium;* [j] *Drug Development Unit, Institute of Cancer Research and the Royal Marsden NHS Trust, Surrey, UK*

Article info

Article history:
Accepted June 29, 2016

Associate Editor:
James Catto

Keywords:
Advanced prostate cancer
Metastatic castrate-resistant prostate cancer
Bone scans
PET/CT scans
Whole-body MRI
Diffusion MRI
Response assessment
Metastasis detection

Abstract

Context: To effectively manage patients with advanced prostate cancer (APC), it is essential to have accurate, reproducible, and validated methods for detecting and quantifying the burden of bone and soft tissue metastases and for assessing their response to therapy. Current standard of care imaging with bone and computed tomography (CT) scans have significant limitations for the assessment of bone metastases in particular.
Objective: We aimed to undertake a critical comparative review of imaging methods used for diagnosis and disease monitoring of metastatic APC from the perspective of their availability and ability to assess disease presence, extent, and response of bone and soft tissue disease.
Evidence acquisition: An expert panel of radiologists, nuclear medicine physicians, and medical physicists with the greatest experience of imaging in advanced prostate cancer prepared a review of the practicalities, performance, merits, and limitations of currently available imaging methods.
Evidence synthesis: Meta-analyses showed that positron emission tomography (PET)/CT with different radiotracers and whole-body magnetic resonance imaging (WB-MRI) are more accurate for bone lesion detection than CT and bone scans (BSs). At a patient level, the pooled sensitivities for bone disease by using choline (CH)–PET/CT, WB-MRI, and BS were 91% (95% confidence interval [CI], 83–96%), 97% (95% CI, 91–99%), and 79% (95% CI, 73–83%), respectively. The pooled specificities for bone metastases detection using CH-PET/CT, WB-MRI, and BS were 99% (95% CI, 93–100%), 95% (95% CI, 90–97%), and 82% (95% CI, 78–85%), respectively. The ability of PET/CT and WB-MRI to assess therapeutic benefits is promising but has not been comprehensively evaluated. There is variability in the cost, availability, and quality of PET/CT and WB-MRI.
Conclusions: Standardisation of acquisition, interpretation, and reporting of WB-MRI and PET/CT scans is required to assess the performance of these techniques in clinical trials of treatment approaches in APC.
Patient summary: PET/CT and whole-body MRI scans have the potential to improve detection and to assess response to treatment of all types of advanced prostate cancer. Consensus recommendations on quality standards, interpretation, and reporting are needed but will require validation in clinical trials of established and new treatment approaches.

* Corresponding author. Paul Strickland Scanner Centre, Mount Vernon Hospital, Rickmansworth Road, Northwood, Middlesex HA6 2RN, UK. Tel.: +44 0 1923 844751; fax: +44 0 1923 844600.
E-mail address: anwar.padhani@stricklandscanner.org.uk (A.R. Padhani).

http://dx.doi.org/10.1016/j.euf.2016.06.018

Please cite this article in press as: Padhani AR, et al. Rationale for Modernising Imaging in Advanced Prostate Cancer. Eur Urol Focus (2016), http://dx.doi.org/10.1016/j.euf.2016.06.018

1. Introduction

Advanced prostate cancer (APC) patients who present with metastatic disease at the time of diagnosis or after failed attempts at curative therapy almost always respond to androgen deprivation therapy (ADT). However, ADT initiation inevitably leads to the development of the castration-resistant disease state, which occurs within 1–3 yr in most patients [1,2]. More than 80% of patients with metastatic castrate-resistant prostate cancer (mCRPC) have bone metastases, which produce significant morbidity and are associated with increased mortality [3–5]. Data from older studies suggest that overall survival (OS) is approximately 30–36 mo from the appearance of metastases, with a median OS of approximately 18 mo once the metastatic castrate-resistant state is established [6–8]. More contemporary data confirm that OS remains poor, approximately 30–42 mo [9–11], even with the increased number of active treatments available for mCRPC. These data emphasise the continued need for improvements in the diagnosis and treatment of APC.

With the increasing availability of therapies that prolong survival for metastatic castrate-naive prostate cancer (PCa) and mCRPC and the increasing use of prostate-specific antigen (PSA) testing after definitive therapy, imaging detection of the metastatic state is occurring for lower disease burdens. Recent data on patients who developed metastatic disease indicated that most have bone-only disease (62%), with bone and soft tissue metastases occurring in an additional 12% [9]. Soft tissue metastases occur mostly in lymph nodes outside the true pelvis, possibly because many patients receive pelvic radiotherapy for biochemical recurrence (BCR). Visceral metastases (liver, lungs, and other sites) occur infrequently at initial relapse (2%) [9], but prevalence increases with advancing disease (15–21% in mCRPC) [12,13]. The prevalence of visceral metastases also increases after multiple lines of treatment and with the emergence of aggressive histologic variants; antemortem, visceral disease can be observed in up to half of the patients [14].

APC patients with bone metastases have a greater risk of skeletal morbidity, which can impair quality of life (QoL) [15]. Bone disease causes pain, pathologic fractures, hypercalcaemia, anaemia, and spinal cord and nerve compression. Delaying symptoms from bone metastases as APC progresses is central to therapeutic management [16]. Treatments for bone metastases are generally systemic but often include local radiotherapy and/or surgery; all are currently given with palliative intent. The treatment of APC with bone metastases has significant health economic implications including the costs of systemic therapy (endocrine therapy, chemotherapy, radioisotope treatments, bisphosphonates, other supportive care medications); imaging; hospital admissions for the treatment of fractures, hypercalcaemia, and cord compression; and the costs of palliative radiotherapy [5,17].

To effectively manage patients with metastatic disease, it is essential to have accurate, reproducible, and validated methods for detecting and assessing response to therapy. These methods include clinical reviews, the use of serum PSA as a tumour marker, circulating tumour cell counts, blood and urinary markers of bone health, and imaging assessments [18,19].

1.1. Need for comprehensive metastatic imaging assessments

Imaging helps define the clinical groups for drug development [20] and clarifies the APC state for therapy recommendations [21] because the presence, volume, and distribution of metastatic disease has profound implications for the curability of PCa, greatly affecting therapy choices. At initial staging or in the setting of initial BCR, for example, the presence of metastatic disease often precludes the use of curative and local salvage options. The time to metastasis development in BCR is also highly prognostic, with a shorter interval to radiographically depicted metastasis associated with poor OS [22]. The presence and volume of metastatic skeletal disease is also highly prognostic, regardless of the imaging method used for metastatic volume estimation [12,23–26].

Imaging can also identify patients with metastatic disease patterns who have poorer prognosis. Subgroup analysis of major clinical trials has shown that imaging features contribute strongly to prognostic models that predict for survival for docetaxel-treated patients [27]. In mCRPC, the location of metastases, particularly the presence of visceral disease and the number of skeletal metastases, are highly prognostic [13,28–30]. A recent meta-analysis showed varying OS according to the anatomic location of metastases in men with mCRPC treated with docetaxel, with increased lethality for lung and liver metastases compared with bone and lymph nodal involvement [13].

Patients with poorer prognosis and higher tumour volumes appear to benefit from intensified combination treatments [12,31,32]. In the CHAARTED study, "high volume" disease was defined by the imaging presence of visceral disease and/or more than four bone metastases with at least one metastasis beyond vertebral bodies or the pelvic skeleton [12]. In mCRPC, the presence of visceral or symptomatic disease is often used as a reason for initiating chemotherapy in fit patients [21,33].

Patients are deemed to have "anaplastic features" based on clinical, biochemical, or imaging results. Imaging features used include exclusively visceral or predominantly lytic bone metastases, bulky tumour masses, low PSA levels relative to tumour burden, and short responses to ADT. Patients defined in this way may benefit more from combination docetaxel and platinum chemotherapy compared with docetaxel alone [31], although this remains controversial.

Well-powered clinical studies have shown that that abiraterone and enzalutamide therapy of asymptomatic or mildly symptomatic chemotherapy-naive mCRPC patients can be helpful for delaying clinical decline and death [10,34]. In this group, lower volume disease such as fewer than four bone metastases [30] and better performance status [11,35] seem to indicate improved OS. Note, however, that the presence of visceral disease and/or large-volume

Please cite this article in press as: Padhani AR, et al. Rationale for Modernising Imaging in Advanced Prostate Cancer. Eur Urol Focus (2016), http://dx.doi.org/10.1016/j.euf.2016.06.018

nodal metastases also precludes the use of some treatments such as the alpha particle emitter radium 223 [36].

Finally, the duration of imaging responses is also reported to be highly prognostic. No response or shorter durations of response to abiraterone and docetaxel treatments using bone scans (BSs) and the size-based criteria (for soft tissue disease) are associated with worse OS [37,38]. These poorer prognosis patients, failing androgen axis–targeted therapies, may benefit from earlier treatment with nontargeted survival-prolonging combination therapies such as docetaxel and cabazitaxel while still asymptomatic, although this too remains controversial.

These data, taken together, emphasise the need for improved precision in evaluating the metastatic status of APC patients, as baseline imaging characteristics can influence therapy choices. Furthermore, these data suggest a need for the detection of metastases when disease load is lower and for more accurate readouts of therapy benefits (to detect primary and secondary resistance) to enable individualised treatment approaches to be investigated.

2. Evidence acquisition

2.1. Search strategy and selection criteria

At the 2015 St. Gallen Advanced Prostate Cancer Consensus Conference (APCCC), most oncologic experts accepted that novel imaging techniques (positron emission tomography [PET]/computed tomography [CT] with different radiotracers and whole-body magnetic resonance imaging [WB-MRI]) are more accurate for lesion detection than conventional imaging with CT and BSs [39]. However, panel members noted that there was considerable variability in the cost, availability, and quality of these imaging modalities. Following the APCCC meeting, an expert panel of radiologists with the largest experience of imaging in APC convened to review the performance merits and limitations of currently used imaging methods. We searched for articles in PubMed on APC and metastatic disease, focusing on detection and response assessments between 2000 and 2015. Although the focus was on imaging metastatic PCa, other tumour types with major malignant bone involvement, including myeloma and breast cancer papers, were also evaluated for relevant data. All papers identified were in the English language and were original scientific papers and review articles. We also searched the references listed for additional relevant papers and conference proceedings. As part of the imaging review, guidelines were formulated on the performance, quality standards, interpretation, and reporting of WB-MRI for the assessment of APC; see the accompanying Metastasis Reporting and Data System–Prostate (MET-RADS-P) publication for the guideline [40].

2.2. Biology of bone disease relevant for imaging

The molecular processes driving PCa cell metastasis to the bone are beginning to be understood [41–43]. In bone, PCa cells mostly cause osteoblastic lesions via the secretion of paracrine factors that stimulate osteoblasts recruitment and function, thereby leading to excess bone formation. Osteoclastic activation at the margins allow metastases to enlarge; the latter mechanism may become dominant in late-state disease. Tumour-matrix interactions affect the imaging phenotype; these interactions are summarised in Supplement 1.

2.3. Current use of imaging in advanced prostate cancer management

The current use of imaging in APC was surveyed at the 2015 St. Gallen APCCC [39]. An international expert consensus panel consisting of PCa specialists who were involved in patient care undertook panel discussions and voted on predefined questions on the use of imaging. While continuing to emphasise the use of bone and CT scans, the APCCC panellists highlighted the need to evaluate newer imaging modalities for early diagnosis and treatment monitoring and to assess their impact on patient outcomes. The APCCC discussions on the current use of imaging in APC are summarised in Supplement 2.

2.4. Comparison of imaging technologies for metastatic disease assessments

Radiologic approaches for metastatic evaluations have specific advantages, including their disease manifestation–specific depiction ability (ie, ability to separately assess prostate, bone, nodal, and visceral disease), noninvasive nature, documentation capability, variable ability for whole-body imaging, resolution flexibility (submillimetre to subcentimetre), ability to depict physiologic and molecular processes within and between lesions and patients, and ability to assess spatial heterogeneity of disease distribution and response. Comprehensive reviews of imaging methods for APC can be found in the literature, and all point out that microscopic metastasis depiction cannot be comprehensively undertaken by any external imaging methods [44,45]. In this review, we only comment on commonly used imaging techniques in the setting of APC, focusing on metastasis detection abilities and response assessment capabilities. In Table 1, we summarised the advantages and limitations of imaging techniques, focusing on the partialities of usage.

2.4.1. Bone scans

Currently, BSs are the mainstay of bone metastatic disease evaluations, including modern extensions such as single-photon emission CT (SPECT) and SPECT-CT [46]. It is important to remember that the uptake of technetium Tc 99m bone-binding radiotracers is related to osteoblastic activity and does not necessarily reflect the full burden of disease within the marrow space (Fig. 1). Compared with modern imaging methods such as choline (CH)–PET/CT and WB-MRI scans, BSs are inferior in terms of lesion detection ability, as discussed in section 3, "Evidence synthesis" [47,48].

BS evaluations of therapy response are also indirect, with sensitivity for disease progression only in most cases.

Please cite this article in press as: Padhani AR, et al. Rationale for Modernising Imaging in Advanced Prostate Cancer. Eur Urol Focus (2016), http://dx.doi.org/10.1016/j.euf.2016.06.018

Table 1 – Summary of the advantages and limitations of whole-body imaging methods suited for advanced prostate cancer evaluations

	Strengths	Weaknesses	Opportunities
CT scan	• Widely available • Easily standardised • Low cost • Fast acquisition • Quantitative assessments (Hounsfield unit) • Ability to characterise bone disease into the spectrum between sclerotic and lytic • Soft tissue and lytic bone metastasis detection and response assessments • Incorporated into clinical practice and trial guidelines	• Does not directly evaluate malignant bone disease when soft tissue is absent • Radiation exposure • Limited local disease evaluations • Subcentimetre nodal characterisation • Cannot visualise infiltrative (nonsclerotic) bone disease • CT "flare" response • Inability to diagnose response/progression in sclerotic bone metastases	• Complementary to PET or whole-body MRI information • Sclerotic change in nonsclerotic lesions as potential response parameter • Lung metastases detection • Lytic vs nonlytic bone metastases subclassification
Bone scan	• Widely available • Easily standardised • Low cost • Incorporated into clinical practice and trial guidelines	• Does not directly evaluate malignant bone disease; reactive osteoblastic uptake only • Longest examination times • Pre- and postexamination care precautions • Radiation exposure to patients and public due to longer half-life of technetium Tc 99m • No ability to assess soft tissue disease • Lower sensitivity and specificity than CT/MRI • Bone scan flare response • No positive benefit criteria (progression only)	• Improved test performance by addition of SPECT/CT capability Development of bone scan index as prognostic biomarker
Sodium fluoride PET/CT	• High sensitivity and relatively good specificity for bone metastases (CT component adds specificity) Medium-length examination times	• Does not directly evaluate malignant bone disease; reactive osteoblastic uptake only • Limited tracer availability • Expensive • Multiple sources of radiation exposure (CT scans and radiotracer) • Some postexamination care precautions (not burdensome) • Limited ability to assess soft tissue disease related to the lower quality of the CT component; used for attenuation correction • Flare response phenomenon • No positive benefit criteria (progression only)	• Development of NaF tumour volume index as prognostic biomarker
Choline PET/CT	• Directly evaluates malignant bone marrow disease • High sensitivity and relatively good specificity for detection of bone and soft tissue metastases • Ability to assess response of bone and soft tissue disease • Objective response parameters (SUV) Medium-length examination times	• Limited tracer availability • Expensive • Multiple sources of radiation exposure (CT scans and 18F-CH radiotracer. less so for 11C-CH due to shorter half-life) • Some postexamination care precautions (not burdensome) • Potential to be influenced by bone marrow–stimulating factors • Inability to accurately assess liver and urinary lesions	• Development of SUV as a potential response biomarker • Development of tumour load as a prognostic biomarker
Whole-body MRI	• Directly evaluates malignant bone marrow disease • Potential wide availability Lack of radiation • Flexible, adaptable imaging (possible to tailor examinations according to disease location) • Ability to detect and assess response of bone and soft tissue disease including the prostate, nodes, and viscera • Objective response parameters (size, volume, and ADC measurements)	• Competing demands for MRI resource • Scanner-dependent performance • Longer acquisition time • Susceptible to artefacts • Subcentimetre nodal and lung metastases detection and characterisation ability • Influenced by bone marrow–stimulating factors and blood transfusions • Limited radiologic expertise in some aspects of image analysis • Data analysis challenges • Higher cost (equal to combined bone and CT scans) and reimbursement challenges	• Radiation-free long-term follow-up • Surgical planning • Skeletal event detection (spinal cord compression, critical fractures) • "One stop-shop": bone and soft tissue disease detection and response assessments

ADC = advanced prostate cancer; CH = choline; CT = computed tomography; MRI = magnetic resonance imaging; PET = positron emission tomography; SPECT = single-photon emission computed tomography; SUV = specific uptake values.

Please cite this article in press as: Padhani AR, et al. Rationale for Modernising Imaging in Advanced Prostate Cancer. Eur Urol Focus (2016), http://dx.doi.org/10.1016/j.euf.2016.06.018

Among the major limitations of BS when assessing therapy effects is the possibility of a "flare" reaction when BSs are performed within 8–12 wk of treatment initiation (flare is defined as the development of new lesions on a first follow-up scan that actually represent a favourable response to treatment on longer term observations [20,49]; the enlargement of previously detected lesions is currently excluded from the definition of the flare reaction in pharmaceutical trials). Such flare reactions can occur in up to 15% of mCRPC patients treated with abiraterone [37]. These flare reactions can lead to diagnostic confusion (pseudoprogression vs true progression) and can result in incorrect management changes [50]. To take into account the possibility of early flare reactions, the Prostate Cancer Clinical Trials Working Group (PCWG) suggested that all patients that have at least two new lesions on the first follow-up BS require a confirmatory BS to be performed after >6 wk while treatment is continued [20,51]; BS progression is documented to have occurred only if two or more new lesions are seen on the confirmatory BS (2 +2 rule) [20]. This means that management change for primary therapy resistance cannot occur until after at least 14 wk of treatment (depending on the reassessment schedule). Readers should also note that the emergence of two or more new lesions after the flare period only requires confirmation on a follow-up scan (ie, new lesions are not required); this strategy can also result in delays in changing therapy in the setting of secondary resistance.

We have already noted that BS progression criteria do not take in consideration increases in extent of preexisting lesions, relying only on the emergence of new lesions [52], further limiting the utility of BS to identify disease progression. Another important point to note is that the PCWG progression criteria described earlier cannot be applied to patients with diffuse metastatic bone disease BS uptake ("superscans"), as new disease cannot be identified on the background of diffusely elevated tracer uptake.

It should also be pointed out that the ability of BS to positively identify response (as opposed to stable or progressive disease) is also constrained because reductions of bone activity take a prolonged period of time to occur, limiting the timeliness of readouts. To date, the rapid resolution of BS is a phenomenon that is almost never observed among therapies known to confer survival benefit; therefore, BS reductions in activity should not be considered as a positive indicator of response. Rapid reductions in BS activity were shown in clinical trials of cabozantinib in APC (Supplementary Fig, 2) [53], but reductions of BS activity did not predict OS [54].

More recent advances in BS lesion quantification such as lesion area, the BS index, or lesion number [25,46,55,56] do not help overcome the limitations of the BS as a tool to identify therapy benefit. However, as already noted, disease load depicted on BS is highly prognostic [12,24,25], and increases in quantitative BS index can be used to identify disease progression in therapy assessment settings [55,57].

To summarise, the clinical consequences of the limited performance of BS readouts when assessing response include (1) inability to diagnose primary and secondary treatment resistance rapidly, keeping patients on treatments from which they may gain no benefit for longer than necessary (overtreatment for nonresponding disease), (2) undertreatment when flare reactions are mistaken for disease progression in responding patients (pseudoprogression vs progression confusion), (3) undocumented increases in tumour burden (increase in extent but not number of bone lesions) while awaiting the emergence of new lesions on confirmatory BS (potentially disadvantaging patients regarding future clinical trials entry). In addition, many patients with bone superscans cannot be evaluated at all. For these reasons, in our opinion, the current evidence points away from the use of BSs for clinical practice when assessing response in bone disease. However, given the wide availability of BS and its acceptance in the oncologic community despite recognised limitations, the BS continues to be recommended, particularly for clinical trials [20,21,39,58].

2.4.2. *Computed tomography*

CT can directly evaluate metastatic disease, providing a means of detecting and measuring lesions, evaluating extent of disease involvement, and quantifying response to treatment of soft tissue disease. Consequently, CT scan measurements are incorporated into clinical care and clinical trials for disease detection and response assessment. It must be appreciated that size-based criteria are severely limited for metastatic nodal disease detection in PCa [59]. However, there is considerable efficacy using CT-based size criteria for assessing therapy response of known soft disease, thus the incorporation of CT measurements into response assessment systems such the PCWG criteria and Response Evaluation Criteria In Solid Tumors (RECIST) [20,60].

CT scans also allow the structure of bone disease to be evaluated, enabling the primary classification of bone metastasis on a spectrum from lytic to sclerotic disease. The biological basis for the range of bone metastasis manifestations is discussed in detail in Supplement 1. It is important to note that patients with CT-depicted presence of predominantly lytic bone metastases associated with bulky soft tissue disease, including visceral disease (in patients with low PSA levels relative to tumour burden), should be considered to have anaplastic features. These patients may require biopsy with a view to reassessing the histologic phenotype and to intensive chemotherapy if anaplastic or neuroendocrine variants are found [31].

Some studies have shown that CT scans are superior to BSs for detecting lytic bone disease and in differentiating between sclerotic changes associated with malignancy versus degenerative disease. Consequently, CT serves as an aid to improve the test performance of BSs (SPECT/CT) and sodium fluoride PET scans (NaF-PET/CT). However, test performance for metastatic detection remains inferior to WB-MRI and PET/CT scans, especially for nonsclerotic, nonlytic bone metastases [47], as detailed in section 3, "Evidence synthesis."

It is accepted that CT scans can be used to assess bone metastasis response to treatment in clinical trials but only

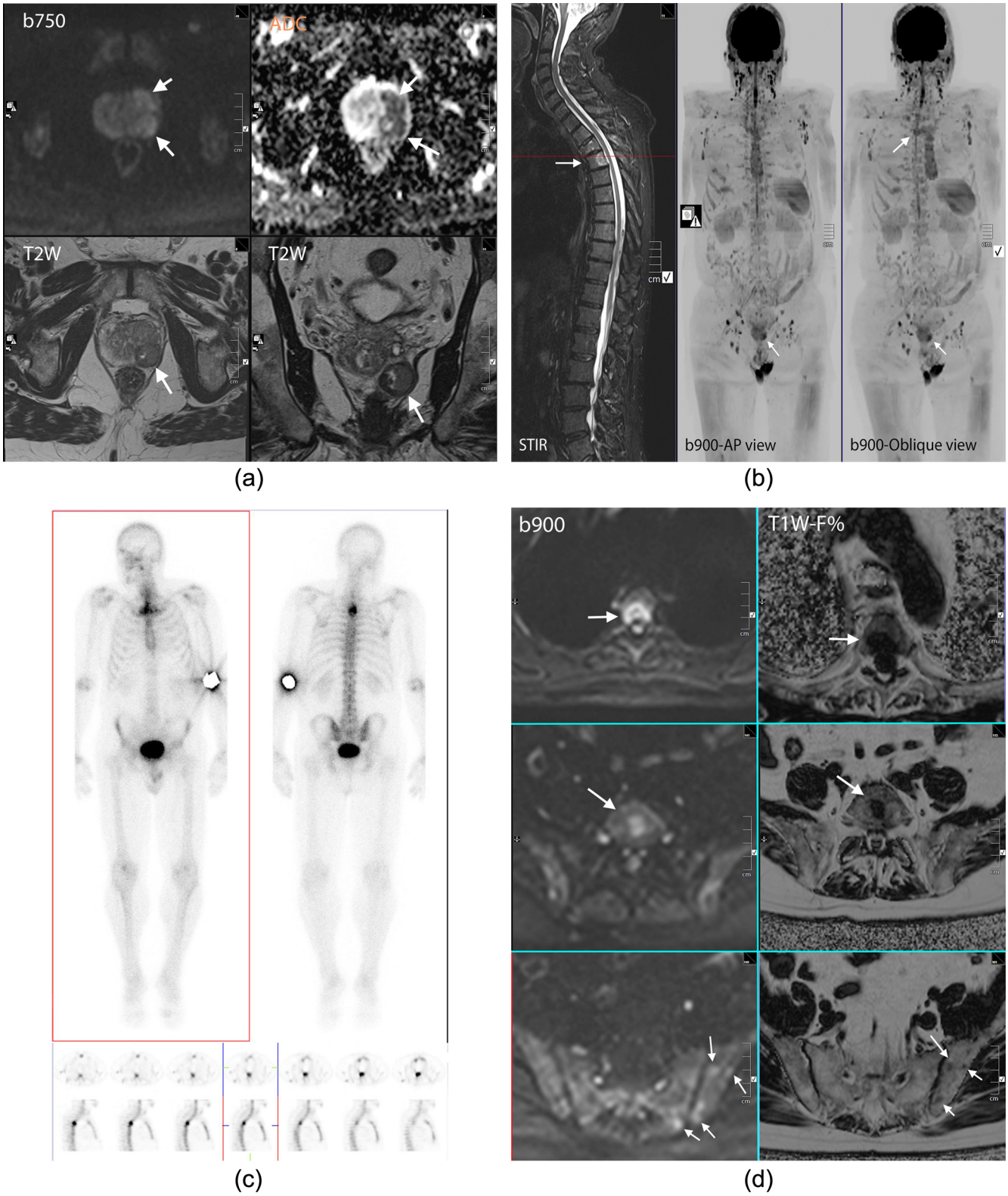

Fig. 1 – Multiregional whole-body magnetic resonance imaging (WB-MRI) capability. Clinical details: A man aged 74 yr with high-risk prostate cancer (prostate-specific antigen 37.5 ng/m; Gleason 4 + 4; five of nine cores positive on the left side only). Clinical question: query local and metastatic staging. (a) Dedicated multiparametric prostate MRI (b value of 750 s/mm^2 [b750], apparent diffusion coefficient map, T2-weighted images in the axial and coronal plane) were undertaken using a 1.5-T scanner. There is a large 4-cm left apical mass bulging the prostatic capsule in the region of the left neurovascular bundle, indicating T3a disease (arrows). (b) Planar (anterior and posterior views) and single-photon emission computed tomography (sagittal and axial sections) bone scans showing the presence of a likely metastasis in the upper dorsal spine. Localisation to a specific vertebral body is difficult. No other lesions were detected. (c) A comprehensive WB-MRI protocol was undertaken using a 3-T scanner (note the higher signal intensity compared with the 1.5-T scanner images in Fig. 3–5 and Supplementary Fig. 2 and 4). Sagittal short tau inversion recovery (STIR) and maximum-intensity projection images (anteroposterior projection and right shoulder forward, oblique) all show a metastasis in the T4 vertebral body

Please cite this article in press as: Padhani AR, et al. Rationale for Modernising Imaging in Advanced Prostate Cancer. Eur Urol Focus (2016), http://dx.doi.org/10.1016/j.euf.2016.06.018

when there is clearly measurable soft tissue disease [20,51,60]. However, the presence of measureable soft tissue occurs in only a minority of bone lesions [61], rendering many patients with bone disease ineligible for trial entry because there are no accepted bone tumour response criteria.

The development of bone sclerosis within metastatic lesions has been suggested as a method for assessing response for metastatic breast cancer within the MD Anderson Cancer Center criteria, provided that bisphosphonates are not used [62]. These criteria recognise that bone structures rarely normalise with effective therapy and that the development of dense osteosclerosis of a lytic or mixed lytic/sclerotic lesion can be used as an indicator of therapy benefit because increased osteoblastic activity occurs as a healing response. However, no CT density thresholds have been established for distinguishing inactive bone metastases from active sclerotic metastases, although emerging data suggest that a well-defined bone lesion with homogenous increased CT density (>800–1000 Hounsfield units) can be relatively inactive when judged on CH-PET/CT scans [63]. The CT flare phenomenon, defined as the emergence of a new bone lesion or a transformational change of an ill-defined sclerotic lesion into a dense, well-marginated bone lesion, has been described in 8% of APC patients and has been successfully treated [64]. The development of new osteosclerotic lesions should not be classified as progression on its own unless there is other evidence of disease progression.

Taking the above discussion into considerations, we suggest that bone disease progression on CT can be identified by the unequivocal presence of new or enlarging soft tissue disease associated with bone lesions or by the rapid disappearance of sclerotic disease due to replacement by visible lytic disease. New sclerotic lesions by themselves do not constitute progression, particularly when dense or well defined. However, the emergence of new woven bone (milky or irregular appearance with ill-defined margins) in previously normal-appearing regions maybe considered as progression in the presence of consistent MRI/PET-depicted abnormalities and/or clinically worsening disease and in the absence of antiosteoclastic treatments (Fig. 2). We assert that early response of bone metastases on CT scans in the absence of extraosseous soft tissue disease cannot be identified but may be seen late when normal trabecular bone is restored.

2.4.3. *Positron emission tomography*

Two PET radiotracers are widely used for imaging APC: the bone-seeking tracer fluorine F 18 (^{18}F)–NaF, which, like 99mTc-MDP, acts as a more efficient marker of osteoblastic action; and the metabolic tracer carbon 11 (^{11}C)/^{18}F–CH, the uptake of which is partially related to membrane phospholipid synthesis [65,66]. There are many other PET tracers, such as fluorodihydrotesterone (directed to the androgen receptor [AR]), gallium- and fluoride-labelled prostate-specific membrane antigen (PSMA), and F-fluciclovine (amino acid transportation; approved by the US Food and Drug Administration in 2016), that have variable geographic availability and for which assessment of clinical utility for disease detection and response in APC is ongoing [67]. The more commonly used general oncology radiotracer fluorodeoxyglucose (FDG-PET/CT) is not often used in the evaluation of APC because of its low sensitivity for disease detection [68]. However, it has been reported that in APC patients with FDG-avid metastases, the amount and extent of FDG-avid disease inversely correlate with survival [61].

CH-PET has potential advantages in displaying changes in metabolic activity that may occur prior to changes in CT-depicted morphology [63]. CH-PET/CT scans are superior to BSs and CT scans for detecting bone disease, with performance equivalent to WB-MRI scans [48]. CH-PET/CT performs poorly in the liver because there is high background hepatic uptake, limiting potential use for later stages of mCRPC, when there is an increased prevalence of metastatic liver disease [14]. In addition, ^{18}F-CH–PET/CT performs poorly in the evaluation of the urinary tract due to urinary excretion (not seen with ^{11}C-CH). In contrast, CH-PET/CT performs better than WB-MRI in the assessment of lymph nodes [48] (Supplementary Fig. 3), although there are limitations in detecting microscopic disease in normally sized nodes at low serum PSA levels (<0.5–1.0 ng/ml in prostatectomy patients) [69]. The ability of CH-PET/CT to assess response has not been systematically evaluated, but a few small studies have shown changes in disease extent and specific uptake values in response to treatment [23,63,70] (Fig. 3). It should also be noted that the flare phenomenon (false increases in fluorocholine PET tracer uptake) can also be observed in responding bone lesion early after starting abiraterone [70].

Preliminary data suggested that PSMA-targeted *N*-(*N*-[(*S*)-1,3-dicarboxypropyl]carbamoyl)-4-^{18}F-fluorobenzyl-L-cysteine (^{18}F-DCFBC) PET/CT has improved performance compared with CT and BS for disease detection [71]. Early data also suggested that the more frequently used gallium Ga 68 PSMA radiotracers have greater sensitivity for disease detection than CH-PET/CT in patients with BCR, especially at low PSA values, although test performance remains dependent on PSA levels [72–74]. The improved performance of PSMA-PET/CT compared with CH-PET/CT is possibly caused by lowered background activity in the bones and liver [73,75]. The ability of PSMA-PET/CT to evaluate therapy response has not been systematically

(arrow). The lower signal in centre of the lesion on the STIR image is consistent with mineralisation. There is osteoporotic loss of vertebral height at T3. The primary tumour at the left prostatic apex is also visible (arrows). (d) (left column) B value of 900 s/mm^2 (b900) diffusion-weighted and (right column) T1-weighted fat-fraction images confirm the presence of the metastasis at T3 (top row; arrow). Further metastases are seen at L5 (middle row; arrow), and multiple smaller lesions are in the left posterior iliac bone (bottom row; arrows). Note the lower lesion contrast on the diffusion-weighted b900 images of the L5 and iliac bone lesions.

ADC = apparent diffusion coefficient; AP = anteroposterior; b750 = b value of 750 s/mm^2; b900 = b value of 900 s/mm^2; STIR = short tau inversion recovery; TW1 = T1 weighted; T2W = T2 weighted.

Please cite this article in press as: Padhani AR, et al. Rationale for Modernising Imaging in Advanced Prostate Cancer. Eur Urol Focus (2016), http://dx.doi.org/10.1016/j.euf.2016.06.018

Fig. 2 – Bone disease progression criteria. A man aged 74 yr with metastatic castrate-resistant prostate cancer was treated with abiraterone. Increasing symptoms with nausea and bone pain were accompanied by a rise in serum prostate-specific antigen. Computed tomography scans before and during treatment. Software straightening and vertebral body labelling of the lumbar spine was undertaken for illustration purposes. There is evidence of disease progression due to the presence of new woven bone (milky or irregular appearance with ill-defined margins) in previously normally appearing regions in the lumbar spine and sacrum with loss of height in several vertebrae.
PSA = prostate-specific antigen.

evaluated. In this context, it must also be remembered that PSMA expression is dependent on the AR status of PCa cells, and the way in which AR-directed treatments alter PSMA-PET/CT test sensitivity remains largely unexplored [76,77].

2.4.4. *Magnetic resonance imaging*

MRI can also directly evaluate metastatic disease, providing a means of detecting and measuring lesions, evaluating the extent of disease involvement, and quantifying response to treatment of both soft tissue and bone marrow disease. Consequently, MRI scan measurements are incorporated into clinical care and clinical trials for disease detection and response assessment, often as alternatives to CT scans. CT detection is superior for lung metastasis, but MRI performs better in detecting liver lesions. As with CT, size-based criteria severely limit metastatic nodal disease detection in PCa [59].

The key advantage of MRI is that bone marrow disease is directly evaluated. MRI sequences can be designed to be sensitive to different aspects of the marrow, such as marrow water and fat (using proton density–weighted, T1-weighted [T1W], T2-weighted [T2W], and short τ inversion recovery [STIR] sequences), the cellularity of the bone marrow (diffusion-weighted [DW] MRI), vascularity (dynamic contrast-enhanced MRI), trabecular bone (ultrashort echo time MRI and susceptibility weighted MRI), and bone marrow fat:water ratio (Dixon MRI, magnetic resonance spectroscopy). Importantly, techniques can be combined within the same examination to enable both morphologic and functional (including quantitative) assessments that can be repeated as often as required, as there is no radiation exposure penalty. Another advantage of MRI is the ability to perform disease-tailored multiregional studies focused on the bones, lymph nodes, viscera, and prostate gland

Please cite this article in press as: Padhani AR, et al. Rationale for Modernising Imaging in Advanced Prostate Cancer. Eur Urol Focus (2016), http://dx.doi.org/10.1016/j.euf.2016.06.018

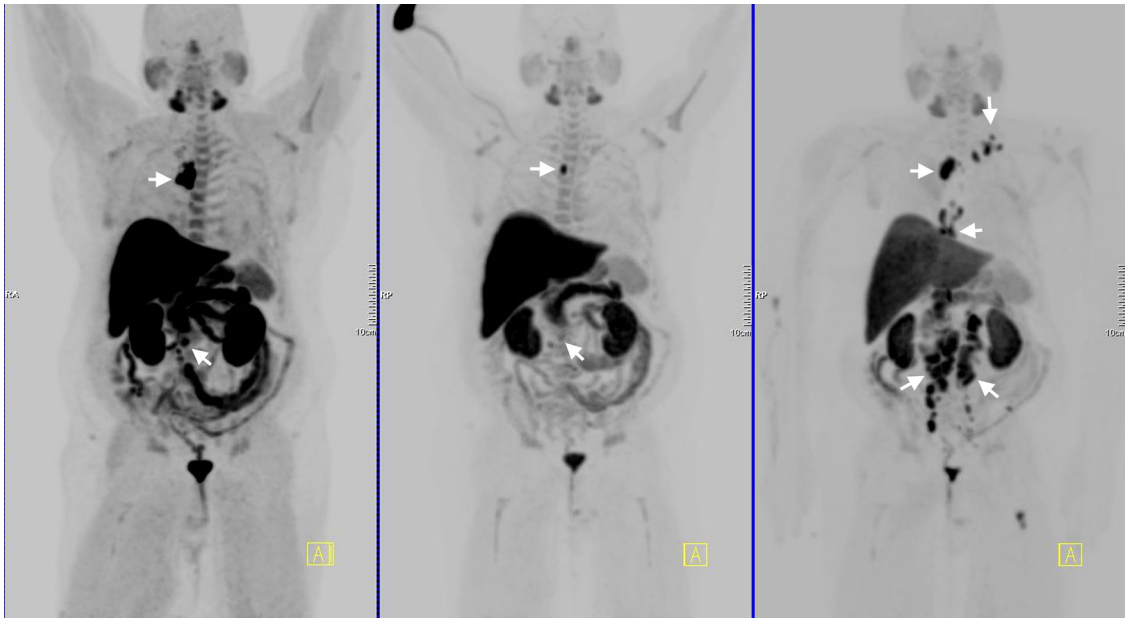

Fig. 3 – Choline positron emission tomography (PET) to monitor response to chemotherapy. A man aged 57 yr with metastatic castrate-resistant prostate cancer. Fluorocholine PET scans (frontal projection, inverted scale). Note normal high radiotracer uptake in liver, kidneys, urinary bladder, pancreas, small bowel, salivary glands, and pituitary fossa. (Left panel) Status after abiraterone and docetaxel (prostate-specific antigen [PSA] 5.2 ng/ml) showing mediastinal (horizontal arrow) and retroperitoneal (slanting arrow). (Middle panel) After six cycles of cabazitaxel chemotherapy (PSA 3.2 ng/ml), the patient showed a good response with residual abnormalities. (Right panel) Extensive relapsed disease on follow-up (PSA 133 ng/ml) with extensive subdiaphragmatic nodal relapse together with left supraclavicular nodal disease (vertical down arrow). New metastasis in the left upper femur. Note fading of background bone marrow due to cell kill effects of chemotherapy.

(Fig. 1). A WB-MRI examination suitable for disease detection and response assessment can be performed in <1 h; practical WB-MRI sequence protocols can be found in the accompanying MET-RADS-P standards publication [40].

2.4.4.1. Morphologic magnetic resonance imaging scans. Morphologic T1W, T2W, and STIR images can be easily acquired on all MRI scanners without exception, and radiologic expertise for their interpretation is widely available [78,79]. Morphologic sequences are key for the confident detection of new metastases until the time when diffuse disease occurs, after which the detection of disease reactivation becomes problematic. Morphologic criteria for bone disease progression and response are well described in the literature [78]. Small studies in metastatic breast cancer have described morphologic MRI bone marrow changes in response to treatment [80,81]. A study evaluating 109 MRI studies in advanced breast cancer found that it was possible to accurately predict progression in 79% of cases and stable disease in 75% of cases, but MRI could not predict regression of disease due to the limitations of morphologic sequences [81]. Specific clinical data on the use of morphologic MRI in the routine assessment of metastatic bone disease response in APC are lacking [82]. Tombal et al noted that there was an opportunity to measure bone disease using morphologic MRI sequences (disease that would otherwise be considered unmeasurable by RECIST) and, in so doing, to potentially double the proportion of APC patients who could be entered into clinical trials [83]. This suggestion of RECIST-like criteria for bone disease assessment has not been widely taken up nor validated in clinical trials.

Morphologic MRI sequences that assess bone marrow response have a number of limitations, including arrested resolution of abnormalities despite effective therapy (the *residual scar* phenomenon, presumed to be due to bone sclerosis, marrow fibrosis, or tumour necrosis) [81]. Another limitation is the problem of evaluating disease activity on a background of previously treated disease (ie, progression can be documented only by the emergence of new disease on previously uninvolved marrow). A T1W image pseudoprogression, the flare phenomenon, can also occur because of intense bone marrow oedema following tumour cell kill and inflammation. T1W flare is more likely to be associated with chemotherapy use and, locally, after radiation treatment, but its frequency is undocumented.

2.4.4.2. Diffusion-weighted images. The disease detection and response assessment performance of WB-MRI is enhanced by adding DW sequences [84–86], which also help to overcome some of the limitations of morphologic sequences, described earlier. DW images depict the per-pixel averages (ie, at millimetre scale) of microscopic tissue water mobility. Modified fat-suppressed T2W sequences are adapted by adding sets of magnetisation gradients that, depending on their timing and magnitude (denoted as the b value, in seconds per square millimetre), induce sensitisation to tissue water diffusion in the resulting images. The water diffusivity can be calculated (apparent diffusion coefficient [ADC] value, in square micrometres per second) [87] and reflects the freedom of water movement. At the cellular

Please cite this article in press as: Padhani AR, et al. Rationale for Modernising Imaging in Advanced Prostate Cancer. Eur Urol Focus (2016), http://dx.doi.org/10.1016/j.euf.2016.06.018

level, water mobility is determined by tissue architectural properties such as cellular density, cellular arrangements, vascularity and extracellular space, tissue viscosity, and tortuosity. A negative correlation between cellular density and ADC value is usually found in soft tissue tumours [88]. Similarity, negative correlations between PCa tumour proliferation and ADC values have been recorded [88,89].

Two kinds of images are produced from diffusion sequences: a set of qualitative DW images (one for each b value) and one quantitative ADC map, both of which need to be assessed. High–b value images are often reconstructed (using maximum-intensity projections) to appear "PET-like," wherein the distribution of malignant disease appears bright (or dark on inverted grey-scale images) (Fig. 1 and 3–5; Supplementary Figs. 2–4). On whole-body DW imaging (WB-DWI), infiltrative skeletal metastases appear as focal or diffuse areas of high signal intensity on high–b value images on a background of the lower signal intensity of the normal bone marrow [86,90,91].

It is important to emphasise that metastasis depiction by WB-DWI should always be correlated with appearances on complementary anatomic sequences to avoid false results [92,93]. Correlations of signal intensity on high–b value images with ADC measurements is especially important for bone lesion characterisation. ADC values of normal marrow are lower than those of metastases due to the presence of marrow fat, with a cut-off value between 600 and 700 $\mu m^2/s$ [94–96] when b values between 50 and 900 s/mm^2 are used. Recommended cut-off values between normal marrow and tumour are set out in detail in the MET-RADS-P standards document [40].

Recently, Perez-Lopez et al. described a semiautomated segmentation tool to derive tumour volume estimates from high–b value images and to obtain global tumour ADC histograms. Tumour volume measurements from WB-DWI undertaken in this way have been shown to be prognostic in APC [26]. Whole-body tumour volumes and ADC histograms can also be used to assess disease response to therapy [97], as illustrated in Fig. 4 and Supplementary Figure 2 and 4. The process of tumour cell lysis and apoptosis disrupts cellular membranes, increasing tissue water diffusivity and thus reducing the signal intensity on high–b value images and increasing ADC values [98–100].

3. Evidence synthesis

3.1. Metastasis detection

Several meta-analyses have shown that the performance of WB-MRI for bone and soft tissue disease detection is comparable to that of FDG-PET/CT, both being significantly more accurate than BS and CT in majority of solid cancers on per-patient and per-lesion bases [47,48,86,101]. Yang et al showed that for all metastatic disease detection on a per-patient basis, the pooled sensitivity estimates for FDG-PET/CT, CT, WB-MRI, and BS were 89.7%, 72.9%, 90.6%, and 86.0%, respectively. The pooled specificity estimates for FDG-PET/CT, CT, WB-MRI, and BS were 96.8%, 94.8%, 95.4%, and 81.4%, respectively [47].

The improved test performance of WB-MRI applies to skeletal assessments in APC specifically when CH-PET/CT is used as the comparator technique. Shen et al conducted a meta-analysis of 27 studies in APC and showed that MRI was superior to CH-PET/CT and BS for metastasis detection on a per-patient basis. On a per-patient basis, the pooled sensitivities for bone disease using CH-PET/CT, WB-MRI, and BS were 91% [95% confidence interval [CI], 83–96], 97% (95% CI, 91–99), 79% (95% CI, 73–83), respectively. The pooled specificities for bone metastasis detection using CH-PET/CT, WB-MRI, and BS were 99% (95% CI, 93–100), 95% (95% CI, 90–97), and 82% (95% CI, 78–85), respectively. [48]. In a per-lesion analysis, CH-PET/CT had a higher diagnostic odds ratio that exceeded both BS and bone SPECT for detecting bone metastases.

A recent meta-analysis underscored the usefulness of DWI as a method that improves the detection of bone metastases. Liu et al. [86] evaluated 32 studies with 1507 patients and showed pooled sensitivity, specificity, and area under the curve for DWI of 95% (95% CI, 90–97), 92% (95% CI, 88–95), and 0.98, respectively, on a per-patient basis and 91% (95% CI, 87–94), 94% (95% CI, 90–96), and 0.97, respectively, on a per-lesion basis.

When evaluating the results of the above meta-analyses and, indeed, in all studies reporting test performance, readers should note that intrinsic verification biases are particularly prevalent at lesion-level analyses because it is simply not possible to obtain histopathology for every bone lesion detected, for ethical and practical clinical reasons [102,103]. Consequently, most studies use combinations of imaging methods and/or follow-up as the standards of reference. Furthermore, as with all external imaging methods, microscopic metastasis depiction cannot be comprehensively undertaken.

3.2. Response assessment

Both preclinical and small-scale clinical studies indicate that DWI can be useful for the assessment of therapy response in malignant bone marrow disease in PCa. Preclinical mouse model studies of osseous PCa have shown increases in ADC values with therapeutic success. A mouse model of PCa bone metastases, for example, demonstrated increased ADC values in response to chemotherapy [104]. ADC increases were also noted in PCa bone metastases models treated with combination docetaxel and anti-CCL2 therapy [105] and with cabozantinib [106].

Few systematic studies have been done in PCa patients with bone disease in response assessment settings [94,107]; there are many case series in the context of methodology development [97,100] and assessments of bone disease response when involvement occurs by other malignancies. The study of Reischauer et al, for example, found that mean ADC values of lesions increased significantly after hormonal therapy, in keeping with successful responses gauged by PSA declines [107]. Slight ADC elevations were also noted in nonresponders, but these increases were <20%, whereas ADC increases in responders were of greater magnitude. Interestingly, there was also noticeable spatial heterogeneity

Please cite this article in press as: Padhani AR, et al. Rationale for Modernising Imaging in Advanced Prostate Cancer. Eur Urol Focus (2016), http://dx.doi.org/10.1016/j.euf.2016.06.018

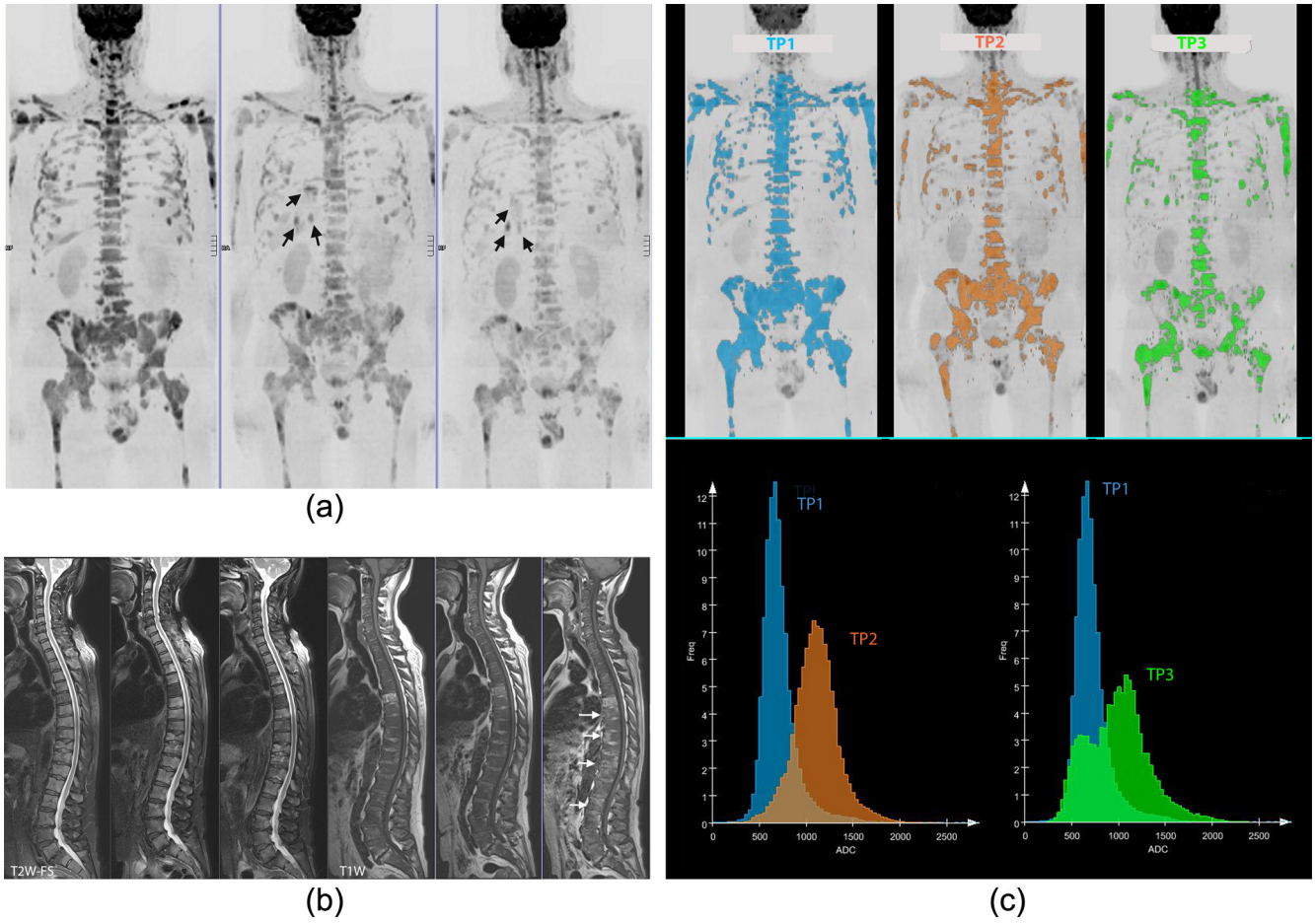

Fig. 4 – Monitoring therapy response to docetaxel chemotherapy. Clinical details: A man aged 76 yr with metastatic castrate-resistant prostate cancer treated with docetaxel chemotherapy. Examinations were obtained at baseline (prostate-specific antigen [PSA] 427 ng/ml) and after three cycles (PSA 301 ng/ml) and six cycles (PSA 136 ng/ml). Clinical question: extent of tumour response. Whole-body magnetic resonance imaging (MRI) scans were performed using a 1.5-T scanner. (a) Diffusion-weighted MRI with a b value of 900 s/mm^2 (b900) and maximum-intensity projection (inverted grey scale, anterior projections) at the three time points (TPs; baseline [TP1] and after three [TP2] and six [TP3] cycles of docetaxel). Extensive bone disease was detected as decreasing in extent and intensity over the three TPs; residual bone disease can still be seen at TP3. Note the emergence of liver metastases (arrows) at TP2 that remain at TP3. (b) T2-weighted fat-saturation (T2W-FS) and T1-weighted (T1W) MRI at the three TPs. Very little change was observed in the T2W-FS images, but increased bone fat can be seen in the lower thoracic and lumbar spine on T1W images at TP3 (arrows); this is consistent with some response to treatment. (c) Segmented whole-body b900 MRI images at the three TPs, using signal normalisation across TPs and identical signal intensity thresholds. Corresponding apparent diffusion coefficient (ADC) histograms for the three TPs, in each case compared with TP1. The *x*-axis is the ADC value (in micrometres per second), and the *y*-axis is the relative frequency. TP1 (blue): 1142 ml of tumour is segmented. The histogram is unimodal with high kurtosis (mean ADC 712 μm^2/s, kurtosis 10.1). TP2 (orange): 500 ml of tumour is segmented. The histogram is still unimodal but moves to the right and decreases kurtosis (mean ADC 1107 μm^2/s, kurtosis 4.1). This finding is in keeping with therapy response. TP3 (green): 360 ml of tumour is segmented. The histogram is now bimodal with the left peak corresponding in value to TP1, and the right peak remains at the value seen at TP2. The failure in the histogram to move further to the right at TP3, together with findings on the other images (liver metastases, persistent abnormalities on morphologic sequences), indicates nonresponse to treatment (secondary resistance). Docetaxel treatment was terminated, and enzalutamide treatment commenced. Image analysis was performed using prototype software (syngo.via Frontier MR Total Tumor Load; Siemens Healthcare, Erlangen, Germany).
TW1 = T1 weighted; T2W-FS = T2-weighted fat saturation; TP = time point.

within individual metastases, with the centre of the lesions having greater increases in ADC values, and variations between metastases in individual patients. Similar findings of increased ADC values in bone disease have been described for multiple myeloma, myeloproliferative diseases, breast cancers, and primary bone tumours with a variety of treatments, indicating that bone tumour ADC increases with successful treatment is a generic finding [108–117]. This matches similar observations made in other organ systems [118].

3.3. *Recommendations*

Our review indicates that both WB-MRI and CH-PET/CT are suitable for wide deployment in disease detection settings, given their test performance, potential wide availability, and multiorgan evaluation capabilities. Sufficient data now indicate that WB-MRI has better accuracy for detecting bone metastases than BS to confidently recommend use for bone metastasis detection. Although further data, including comparative multimodal studies, are

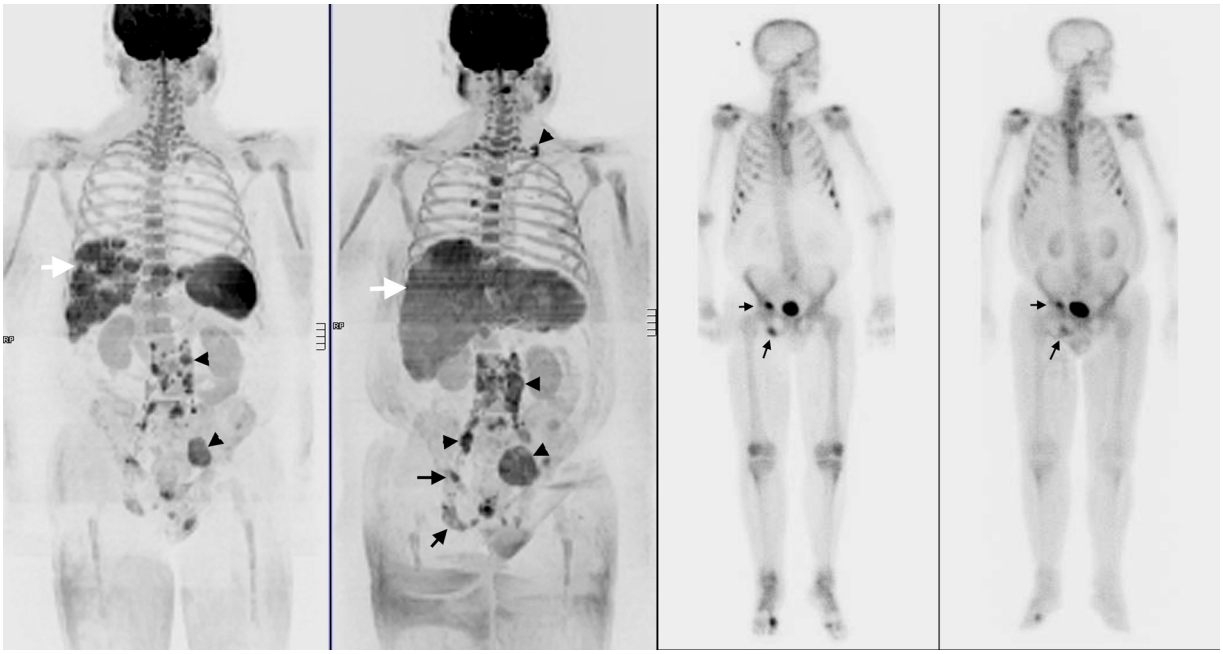

Fig. 5 – Monitoring soft tissue disease therapy response. Clinical details: A man aged 68 yr with metastatic castrate-resistant prostate cancer after docetaxel and abiraterone, treated with mitoxantrone and prednisone. Examinations were obtained at baseline (prostate-specific antigen [PSA] 259 ng/ml) and after 12 wk of treatment (PSA 6093 ng/ml). Clinical question: query evidence of tumour response. whole-body magnetic resonance imaging scans were performed using a 1.5-T scanner. (Left panels) Diffusion-weighted images with a b value of 900 s/mm^2 (b900) and inverted maximum-intensity projection (anterior projections). (Right panels) Planar bone scans (anterior view) at the corresponding time points. Extensive liver disease (horizontal white arrows) is visible, increasing in extent over 12 wk, indicating disease progression. There is lymph nodal disease progression (black arrowheads) within the abdomen and pelvis, including new nodal disease in the left supraclavicular fossa. There was no change in the bone deposits on the diffusion or bone scans (black arrows). Note increased lower limb lymph oedema visible on both scan types. Further active treatment was terminated.

awaited in treatment-response assessment settings, a recent European Organisation for Research and Treatment of Cancer position paper also concluded that MRI offers a good "one size fits all" solution for patients who do not have substantial nonbone disease to assess therapy effectiveness [82].

The St. Gallen APCCC panellists correctly asked whether earlier detection of metastatic disease using highly sensitive imaging methods like WB-MRI and PET/CT will have significant clinical benefits in terms of significant impacts on QoL and OS [39]. Similarly, they asked whether earlier detection of treatment failure or primary resistance by more sensitive methods, and subsequent modifications in life prolonging treatments, would have benefits in terms of maintaining QoL and improving OS. These questions are worth investigating because there are indications that earlier, timely detection and treatment initiation in oligometastatic APC may be beneficial [119]. Some approved treatments are more suited to lower volume disease (local treatments such as surgery and targeted radiation, treatments targeting the androgen axis, and systemic immunotherapy). Furthermore, some treatments may work better when used in asymptomatic or minimally symptomatic patients with better performance status [30,34,35,120]. Emerging guidelines are beginning to recommend prospective screening for metastatic disease in asymptomatic PCa patients, with a view to earlier initiation of treatments and clinical trial entry in oligometastatic disease, and in the setting of nonmetastatic CRPC [20,121,122]. To date, however, there are few data on the benefits of treatment modifications based on the earlier detection of treatment failure or primary resistance and on the negative QoL effects of continued treatments with ineffective drugs [39].

The cost of WB-MRI and PET/CT are often highlighted as a hindrance for clinical adoption in some health systems. However, costs are dependent on the availability of these technologies. Generally, within Europe, the cost of WB-MRI is comparable to the combined costs of CT and BS for the detection of bone and nodal metastases (Table 1) [123,124]. Furthermore, because WB-MRI costs are largely determined by in-room table time, which is rapidly decreasing as MRI machine performance improves, we can expect to see WB-MRI scan times decrease.

There is a recognised need for standardisation of acquisition, interpretation, and reporting of WB-MRI [39]. The MET-RADS-P imaging recommendations have been developed to address these needs [40]. The WB-MRI methods proposed can be adapted for use in advanced metastatic breast cancer (MET-RADS-B) and for multiple myeloma (MET-RADS-MM); in passing, readers should note that WB-MRI is already recommended as the first-line tool for investigation in myeloma [125]. The proposed MET-RADS-P system is suitable for clinical practice and can be incorporated into clinical trials, generating measures that can serve as new biomarkers, which in turn will require independent validation [20].

Please cite this article in press as: Padhani AR, et al. Rationale for Modernising Imaging in Advanced Prostate Cancer. Eur Urol Focus (2016), http://dx.doi.org/10.1016/j.euf.2016.06.018

Initially, we suggest that WB-MRI be evaluated in clinical trials that assess the effects of treatments that are anticipated or known to kill tumour cells, such as those targeting the androgen axis, cytotoxic chemotherapy, and radium 223. More novel trials could include targeted radiotherapy for oligometastases, PARP inhibitors, and immunotherapies. In these studies, WB-MRI should be compared with current criteria (eg, changes in PSA, other biochemical markers, circulating tumour cells) and correlated to QoL measures, rates of skeletal events, and progression-free survival, so as to justify the inclusion of WB-MRI in future studies. Comparative clinical studies of test performance against established and emerging PET radiotracers would also be of interest. The latter are prerequisites for the successful introduction of WB-MRI into longer term follow-up studies that prospectively collect appropriate metadata that would allow objective assessments of whether WB-MRI is effective in directing patient care and supporting drug development.

4. Conclusions

Imaging techniques including WB-MRI and PET/CT scans have the potential to address the unmet need for robust imaging methods that allow tumour detection and therapy evaluations in APC. WB-MRI can detect bone metastases with higher sensitivity than BSs and with performance at least comparable to that of CH-PET/CT. Early and more accurate detection of tumour burden may have positive therapy implications. Importantly, WB-MRI provides clearer categorisation of bone metastasis response, unlike BSs, which only identify disease progression; more accurate assessments of therapy response (including heterogeneity of response) could further aid the rational development of targeted therapies.

There is a clear need for standardisation of WB-MRI and PET/CT technologies. The proposed MET-RADS-P system [40] enables complete characterisation of APC state using WB-MRI not only at the start of treatments but also over time as the disease evolves. MET-RADS-P allows the categorisation of patients with specific patterns of disease for clinical trial stratification. MET-RADS-P also enables the evaluation of the benefits of continuing therapy when there are signs that the disease is progressing (discordant responses). Clearly, WB-MRI is not at the point where it can support regulatory approvals of new therapeutic approaches. It is anticipated that as evidence accrues from clinical trials, more specific recommendations and/or algorithms incorporating WB-MRI and PET/CT will emerge. We recommend that WB-MRI and the MET-RADS-P system now be evaluated in clinical trials to assess the impact on the clinical management of APC.

Author contributions: Anwar R. Padhani had full access to all the data in the study and takes responsibility for the integrity of the data and the accuracy of the data analysis.

Study concept and design: Padhani, Lecouvet, Tunariu, Koh, De Keyzer, Collins, Sala, Schlemmer, Petralia, Vargas, Fanti, Tombal, de Bono.
Acquisition of data: Padhani, Lecouvet, Tunariu, Koh, De Keyzer, Collins.
Analysis and interpretation of data: Padhani, Lecouvet, Tunariu, Koh, De Keyzer, Collins, Sala, Schlemmer, Petralia, Vargas, Fanti, Tombal, de Bono.
Drafting of the manuscript: Padhani, Lecouvet, Tunariu, Koh, De Keyzer, Collins, Vargas, Fanti.
Critical revision of the manuscript for important intellectual content: Schlemmer, Petralia, Tombal, de Bono.
Statistical analysis: Padhani, Lecouvet.
Obtaining funding: None.
Administrative, technical, or material support: None.
Supervision: Tombal, de Bono.
Other (specify): None.

Financial disclosures: Anwar R. Padhani certifies that all conflicts of interest, including specific financial interests and relationships and affiliations relevant to the subject matter or materials discussed in the manuscript (eg, employment/affiliation, grants or funding, consultancies, honoraria, stock ownership or options, expert testimony, royalties, or patents filed, received, or pending), are the following: Anwar R Padhani, Dow-Mu Koh, and David J. Collins have research agreements and speakers bureau declarations for Siemens Healthcare, an imaging company.

Funding/Support and role of the sponsor: We are grateful to the following funding agencies for funding our work: FRS-FNRS Televie, Fondation Contre le Cancer, Fondation Saint Luc (Belgium), and Memorial Sloane Kettering Cancer Center (Support Grant/Core Grant P30 CA008748). We also acknowledge support from Prostate Cancer UK and Movember to the London Movember Prostate Cancer Centre of Excellence at the Institute of Cancer Research and Royal Marsden and through an Experimental Cancer Medical Centre (ECMC) grant from Cancer Research UK and the Department of Health (Ref: C51/A7401). The authors acknowledge UK National Health Service funding to the National Institute for Health Research Biomedical Research Centre at the Royal Marsden and the Institute of Cancer Research. The funders played no role in the decision to undertake this review, the preparation of the manuscript, or the decision to submit the paper for publication.

Acknowledgments: We thank Aurelius Omlin and Silke Gillessen for their helpful clinical insights.

Appendix A. Supplementary data

Supplementary material related to this article can be found, in the online version, at doi:10.1016/j.euf.2016.06.018.

References

[1] Oudard S. Progress in emerging therapies for advanced prostate cancer. Cancer Treat Rev 2013;39:275–89.
[2] Lam JS, Leppert JT, Vemulapalli SN, Shvarts O, Belldegrun AS. Secondary hormonal therapy for advanced prostate cancer. J Urol 2006;175:27–34.
[3] Bubendorf L, Schöpfer A, Wagner U, et al. Metastatic patterns of prostate cancer: an autopsy study of 1,589 patients. Hum Pathol 2000;31:578–83.
[4] Broder MS, Gutierrez B, Cherepanov D, Linhares Y. Burden of skeletal-related events in prostate cancer: unmet need in pain improvement. Support Care Cancer 2015;23:237–47.
[5] Yong C, Onukwugha E, Mullins CD. Clinical and economic burden of bone metastasis and skeletal-related events in prostate cancer. Curr Opin Oncol 2014;26:274–83.
[6] Maximum androgen blockade in advanced prostate cancer: an overview of 22 randomised trials with 3283 deaths in 5710 patients.

Prostate Cancer Trialists' Collaborative Group. Lancet 1995; 346:265–9.
[7] Tannock IF, de Wit R, Berry WR, et al. Docetaxel plus prednisone or mitoxantrone plus prednisone for advanced prostate cancer. N Engl J Med 2004;351:1502–12.
[8] Petrylak DP, Tangen CM, Hussain MHA, et al. Docetaxel and estramustine compared with mitoxantrone and prednisone for advanced refractory prostate cancer. N Engl J Med 2004;351:1513–20.
[9] James ND, Spears MR, Clarke NW, et al. Survival with newly diagnosed metastatic prostate cancer in the 'docetaxel era': data from 917 patients in the control arm of the STAMPEDE trial (MRC PR08, CRUK/06/019). Eur Urol 2015;67:1028–38.
[10] Beer TM, Armstrong AJ, Rathkopf DE, et al. Enzalutamide in metastatic prostate cancer before chemotherapy. N Engl J Med 2014;371:424–33.
[11] Ryan CJ, Smith MR, Fizazi K, et al. Abiraterone acetate plus prednisone versus placebo plus prednisone in chemotherapy-naive men with metastatic castration-resistant prostate cancer (COU-AA-302): final overall survival analysis of a randomised, double-blind, placebo-controlled phase 3 study. Lancet Oncol 2015;16:152–60.
[12] Sweeney CJ, Chen Y-H, Carducci M, et al. Chemohormonal therapy in metastatic hormone-sensitive prostate cancer. N Engl J Med 2015;373:737–46.
[13] Halabi S, Kelly WK, Ma H, et al. Meta-analysis evaluating the impact of site of metastasis on overall survival in men with castration-resistant prostate cancer. J Clin Oncol. In press. http://dx.doi.org/10.1200/JCO. 2015.65.7270
[14] Pezaro CJ, Omlin A, Lorente D, et al. Visceral disease in castration-resistant prostate cancer. Eur Urol 2014;65:270–3.
[15] Bishr M, Saad F. Preventing bone complications in prostate cancer. Curr Opin Support Palliat Care 2012;6:299–303.
[16] Sullivan PW, Mulani PM, Fishman M, Sleep D. Quality of life findings from a multicenter, multinational, observational study of patients with metastatic hormone-refractory prostate cancer. Qual Life Res 2007;16:571–5.
[17] Hoefeler H, Duran I, Hechmati G, et al. Health resource utilization associated with skeletal-related events in patients with bone metastases: Results from a multinational retrospective - prospective observational study - a cohort from 4 European countries. J Bone Oncol 2014;3:40–8.
[18] Horwich A, Hugosson J, de Reijke T, et al. Prostate cancer: ESMO Consensus Conference Guidelines 2012. Ann Oncol 2013;24: 1141–62.
[19] Omlin A, Pezaro C, Gillessen Sommer S. Sequential use of novel therapeutics in advanced prostate cancer following docetaxel chemotherapy. Ther Adv Urol 2014;6:3–14.
[20] Scher HI, Morris MJ, Stadler WM, et al. Trial design and objectives for castration-resistant prostate cancer: updated recommendations from the Prostate Cancer Clinical Trials Working Group 3. J Clin Oncol 2016;34:1402–18.
[21] Castration-resistant prostate cancer: AUA guideline. American Urological Association Web site. https://www.auanet.org/education/guidelines/castration-resistant-prostate-cancer.cfm.
[22] Schweizer MT, Zhou XC, Wang H, et al. Metastasis-free survival is associated with overall survival in men with PSA-recurrent prostate cancer treated with deferred androgen deprivation therapy. Ann Oncol 2013;24:2881–6.
[23] Ceci F, Castellucci P, Graziani T, et al. (11)C-Choline PET/CT in castration-resistant prostate cancer patients treated with docetaxel. Eur J Nucl Med Mol Imaging 2016;43:84–91.
[24] Tait C, Moore D, Hodgson C, et al. Quantification of skeletal metastases in castrate-resistant prostate cancer predicts progression-free and overall survival. BJU Int 2014;114:E70–3.
[25] Sabbatini P, Larson SM, Kremer A, et al. Prognostic significance of extent of disease in bone in patients with androgen-independent prostate cancer. J Clin Oncol 1999;17:948–57.
[26] Perez-Lopez R, Lorente D, Blackledge MD, et al. Volume of bone metastasis assessed with whole-body diffusion-weighted imaging is associated with overall survival in metastatic castration-resistant prostate cancer. Radiology 2016;280. http://dx.doi.org/10.1148/radiol.2015150799
[27] Crawford ED, Higano CS, Shore ND, Hussain M, Petrylak DP. Treating patients with metastatic castration resistant prostate cancer: a comprehensive review of available therapies. J Urol 2015;194:1537–47.
[28] Halabi S, Lin C-Y, Kelly WK, et al. Updated prognostic model for predicting overall survival in first-line chemotherapy for patients with metastatic castration-resistant prostate cancer. J Clin Oncol 2014;32:671–7.
[29] Halabi S, Lin C-Y, Small EJ, et al. Prognostic model predicting metastatic castration-resistant prostate cancer survival in men treated with second-line chemotherapy. J Natl Cancer Inst 2013; 105:1729–37.
[30] Evans CP, Higano CS, Keane T, et al. The PREVAIL study: primary outcomes by site and extent of baseline disease for enzalutamide-treated men with chemotherapy-naïve metastatic castration-resistant prostate cancer. Eur Urol. In press. http://dx.doi.org/10.1016/j.eururo.2016.03.017
[31] Aparicio AM, Harzstark AL, Corn PG, et al. Platinum-based chemotherapy for variant castrate-resistant prostate cancer. Clin Cancer Res 2013;19:3621–30.
[32] James ND, Sydes MR, Clarke NW, et al. Addition of docetaxel, zoledronic acid, or both to first-line long-term hormone therapy in prostate cancer (STAMPEDE): survival results from an adaptive, multiarm, multistage, platform randomised controlled trial. Lancet 2015;6736:1–15.
[33] Mottet N, Bellmunt J, Briers E, et al. Guidelines on prostate cancer. Arnhem, Netherlands: European Association of Urology;; 2015.
[34] Ryan CJ, Smith MR, de Bono JS, et al. Abiraterone in metastatic prostate cancer without previous chemotherapy. N Engl J Med 2013;368:138–48.
[35] Miller K, Carles J, Gschwend JE, Van Poppel H, Diels J, Brookman-May SD. The phase 3 COU-AA-302 study of abiraterone acetate (AA) in men with chemotherapy (CT)-naïve metastatic castration-resistant prostate cancer (mCRPC): stratified analysis based on pain, prostate-specific antigen (PSA) and Gleason score (GS). Eur Urol Suppl 2016;15, abstract 775.
[36] Parker C, Nilsson S, Heinrich D, et al. Alpha emitter radium-223 and survival in metastatic prostate cancer. N Engl J Med 2013;369: 213–23.
[37] Morris MJ, Molina A, Small EJ, et al. Radiographic progression-free survival as a response biomarker in metastatic castration-resistant prostate cancer: COU-AA-302 results. J Clin Oncol 2015;33:1356–63.
[38] Sonpavde G, Pond GR, Templeton AJ, et al. Association between RECIST changes and survival in patients with metastatic castration-resistant prostate cancer receiving docetaxel. Eur Urol 2016;69:980–3.
[39] Gillessen S, Omlin A, Attard G, et al. Management of patients with advanced prostate cancer: recommendations of the St Gallen Advanced Prostate Cancer Consensus Conference (APCCC) 2015. Ann Oncol 2015;26:1589–604.
[40] Padhani AR, Lecouvet FE, Tunariu N, et al. METastasis reporting and data system for prostate cancer: practical guidelines for acquisition, interpretation, and reporting of whole-body magnetic resonance imaging-based evaluations of multiorgan involvement in advanced prostate cancer. Eur Urol 2016. http://dx.doi.org/10.1016/j.eururo.2016.05.033, [Epub ahead of print].

Please cite this article in press as: Padhani AR, et al. Rationale for Modernising Imaging in Advanced Prostate Cancer. Eur Urol Focus (2016), http://dx.doi.org/10.1016/j.euf.2016.06.018

[41] Msaouel P, Pissimissis N, Halapas A, Koutsilieris M. Mechanisms of bone metastasis in prostate cancer: clinical implications. Best Pract Res Clin Endocrinol Metab 2008;22:341–55.
[42] Futakuchi M, Fukamachi K, Suzui M. Heterogeneity of tumor cells in the bone microenvironment: mechanisms and therapeutic targets for bone metastasis of prostate or breast cancer. Adv Drug Deliv Rev 2016;99:206–11.
[43] Hensel J, Thalmann GN. Biology of bone metastases in prostate cancer. Urology 2016;92:6–13.
[44] Beauregard J-M, Pouliot F. New developments in the imaging of metastatic prostate cancer. Curr Opin Support Palliat Care 2014;8:265–70.
[45] Messiou C, Cook G, deSouza NM. Imaging metastatic bone disease from carcinoma of the prostate. Br J Cancer 2009;101:1225–32.
[46] Wong KK, Piert M. Dynamic bone imaging with 99mTc-labeled diphosphonates and 18F-NaF: mechanisms and applications. J Nucl Med 2013;54:590–9.
[47] Yang H-L, Liu T, Wang X-M, Xu Y. Deng S-M. Diagnosis of bone metastases: a meta-analysis comparing 18FDG PET, CT, MRI and bone scintigraphy. Eur Radiol 2011;21:2604–17.
[48] Shen G, Deng H, Hu S, Jia Z. Comparison of choline-PET/CT, MRI, SPECT, and bone scintigraphy in the diagnosis of bone metastases in patients with prostate cancer: a meta-analysis. Skeletal Radiol 2014;43:1503–13.
[49] Ryan CJ, Shah S, Efstathiou E, et al. Phase II study of abiraterone acetate in chemotherapy-naive metastatic castration-resistant prostate cancer displaying bone flare discordant with serologic response. Clin Cancer Res 2011;17:4854–61.
[50] Coleman RE, Mashiter G, Whitaker KB, Moss DW, Rubens RD, Fogelman I. Bone scan flare predicts successful systemic therapy for bone metastases. J Nucl Med 1988;29:1354–9.
[51] Scher HI, Halabi S, Tannock I, et al. Design and end points of clinical trials for patients with progressive prostate cancer and castrate levels of testosterone: recommendations of the Prostate Cancer Clinical Trials Working Group. J Clin Oncol 2008;26:1148–59.
[52] Morris MJ, Autio KA, Basch EM, Danila DC, Larson S, Scher HI. Monitoring the clinical outcomes in advanced prostate cancer: what imaging modalities and other markers are reliable? Semin Oncol 2013;40:375–92.
[53] Brown MS, Chu GH, Kim HJ, et al. Computer-aided quantitative bone scan assessment of prostate cancer treatment response. Nucl Med Commun 2012;33:384–94.
[54] Smith DC, Smith MR, Sweeney C, et al. Cabozantinib in patients with advanced prostate cancer: results of a phase II randomized discontinuation trial. J Clin Oncol 2013;31:412–9.
[55] Dennis ER, Jia X, Mezheritskiy IS, et al. Bone scan index: a quantitative treatment response biomarker for castration-resistant metastatic prostate cancer. J Clin Oncol 2012;30:519–24.
[56] Ulmert D, Kaboteh R, Fox JJ, et al. A novel automated platform for quantifying the extent of skeletal tumour involvement in prostate cancer patients using the Bone Scan Index. Eur Urol 2012;62:78–84.
[57] Armstrong AJ, Kaboteh R, Carducci MA, et al. Assessment of the bone scan index in a randomized placebo-controlled trial of tasquinimod in men with metastatic castration-resistant prostate cancer (mCRPC). Urol Oncol 2014;32:1308–16.
[58] NCCN clinical practice guidelines in oncology (NCCN Guidelines®): prostate cancer version 2.2016. Fort Washington, PA: National Comprehensive Cancer Network; 2016.
[59] Hovels AM, Heesakkers RAM, Adang EM, et al. The diagnostic accuracy of CT and MRI in the staging of pelvic lymph nodes in patients with prostate cancer: a meta-analysis. Clin Radiol 2008;63:387–95.
[60] Eisenhauer EA, Therasse P, Bogaerts J, et al. New response evaluation criteria in solid tumours: revised RECIST guideline (version 1.1). Eur J Cancer 2009;45:228–47.
[61] Vargas HA, Wassberg C, Fox JJ, et al. Bone metastases in castration-resistant prostate cancer: associations between morphologic CT patterns, glycolytic activity, and androgen receptor expression on PET and overall survival. Radiology 2014;271:220–9.
[62] Hamaoka T, Costelloe CM, Madewell JE, et al. Tumour response interpretation with new tumour response criteria vs the World Health Organisation criteria in patients with bone-only metastatic breast cancer. Br J Cancer 2010;102:651–7.
[63] Beheshti M, Vali R, Waldenberger P, et al. The use of F-18 choline PET in the assessment of bone metastases in prostate cancer: correlation with morphological changes on CT. Mol Imaging Biol 2010;12:98–107.
[64] Messiou C, Cook G, Reid AHM, et al. The CT flare response of metastatic bone disease in prostate cancer. Acta Radiol 2011;52:557–61.
[65] Wondergem M, van der Zant FM, van der Ploeg T, Knol RJJ. A literature review of 18F-fluoride PET/CT and 18F-choline or 11C-choline PET/CT for detection of bone metastases in patients with prostate cancer. Nucl Med Commun 2013;34:935–45.
[66] Jadvar H. Prostate cancer: PET with 18F-FDG, 18F- or 11C-acetate, and 18F- or 11C-choline. J Nucl Med 2011;52:81–9.
[67] Fox JJ, Schöder H, Larson SM. Molecular imaging of prostate cancer. Curr Opin Urol 2012;22:320–7.
[68] Jadvar H. Molecular imaging of prostate cancer: PET radiotracers. AJR Am J Roentgenol 2012;199:278–91.
[69] Bauman G, Belhocine T, Kovacs M, Ward A, Beheshti M, Rachinsky I. 18F-fluorocholine for prostate cancer imaging: a systematic review of the literature. Prostate Cancer Prostatic Dis 2012;15:45–55.
[70] De Giorgi U, Caroli P, Burgio SL, et al. Early outcome prediction on 18F-fluorocholine PET/CT in metastatic castration-resistant prostate cancer patients treated with abiraterone. Oncotarget 2014;5:12448–58.
[71] Rowe SP, Gage KL, Faraj SF, et al. 18F-DCFBC PET/CT for PSMA-based detection and characterization of primary prostate cancer. J Nucl Med 2015;56:1003–10.
[72] Afshar-Oromieh A, Haberkorn U, Eder M, Eisenhut M, Zechmann CM. [68Ga]Gallium-labelled PSMA ligand as superior PET tracer for the diagnosis of prostate cancer: comparison with 18F-FECH. Eur J Nucl Med Mol Imaging 2012;39:1085–6.
[73] Morigi JJ, Stricker PD, van Leeuwen PJ, et al. Prospective comparison of 18F-fluoromethylcholine versus 68Ga-PSMA PET/CT in prostate cancer patients who have rising PSA after curative treatment and are being considered for targeted therapy. J Nucl Med 2015;56:1185–90.
[74] Eiber M, Maurer T, Souvatzoglou M, et al. Evaluation of hybrid 68Ga-PSMA ligand PET/CT in 248 patients with biochemical recurrence after radical prostatectomy. J Nucl Med 2015;56:668–74.
[75] Freitag MT, Radtke JP, Hadaschik BA, et al. Comparison of hybrid (68)Ga-PSMA PET/MRI and (68)Ga-PSMA PET/CT in the evaluation of lymph node and bone metastases of prostate cancer. Eur J Nucl Med Mol Imaging 2016;43:70–83.
[76] Miyamoto DT, Lee RJ, Stott SL, et al. Androgen receptor signaling in circulating tumor cells as a marker of hormonally responsive prostate cancer. Cancer Discov 2012;2:995–1003.
[77] Liu T, Wu LY, Fulton MD, Johnson JM, Berkman CE. Prolonged androgen deprivation leads to downregulation of androgen receptor and prostate-specific membrane antigen in prostate cancer cells. Int J Oncol 2012;41:2087–92.

Please cite this article in press as: Padhani AR, et al. Rationale for Modernising Imaging in Advanced Prostate Cancer. Eur Urol Focus (2016), http://dx.doi.org/10.1016/j.euf.2016.06.018

[78] Lecouvet FE, Larbi A, Pasoglou V, et al. MRI for response assessment in metastatic bone disease. Eur Radiol 2013;23:1986–97.
[79] Moulopoulos LA, Koutoulidis V. Bone Marrow MRI: A Pattern-Based Approach. Berlin, Germany: Springer; 2014.
[80] Saip P, Tenekeci N, Aydiner A, et al. Response evaluation of bone metastases in breast cancer: value of magnetic resonance imaging. Cancer Invest 1999;17:575–80.
[81] Brown AL, Middleton G, MacVicar AD, Husband JE. T1-weighted magnetic resonance imaging in breast cancer vertebral metastases: changes on treatment and correlation with response to therapy. Clin Radiol 1998;53:493–501.
[82] Lecouvet FE, Talbot JN, Messiou C, et al. Monitoring the response of bone metastases to treatment with magnetic resonance imaging and nuclear medicine techniques: a review and position statement by the European Organisation for Research and Treatment of Cancer imaging group. Eur J Cancer 2014;50:2519–31.
[83] Tombal B, Rezazadeh A, Therasse P, Van Cangh PJ, Vande Berg B, Lecouvet FE. Magnetic resonance imaging of the axial skeleton enables objective measurement of tumor response on prostate cancer bone metastases. Prostate 2005;65:178–87.
[84] Li B, Li Q, Nie W, Liu S. Diagnostic value of whole-body diffusion-weighted magnetic resonance imaging for detection of primary and metastatic malignancies: a meta-analysis. Eur J Radiol 2014;83:338–44.
[85] Wu LM, Gu HY, Zheng J, et al. Diagnostic value of whole-body magnetic resonance imaging for bone metastases: a systematic review and meta-analysis. J Magn Reson Imaging 2011;34:128–35.
[86] Liu L-P, Cui L-B, Zhang XX, et al. Diagnostic performance of diffusion-weighted magnetic resonance imaging in bone malignancy. Medicine (Baltimore) 2015;94:e1998.
[87] Padhani AR, Liu G, Koh DM, et al. Diffusion-weighted magnetic resonance imaging as a cancer biomarker: consensus and recommendations. Neoplasia 2009;11:102–25.
[88] Chen L, Liu M, Bao J, et al. The correlation between apparent diffusion coefficient and tumor cellularity in patients: a meta-analysis. PLoS One 2013;8:e79008.
[89] Renard Penna R, Cancel-Tassin G, Comperat E, et al. Apparent diffusion coefficient value is a strong predictor of unsuspected aggressiveness of prostate cancer before radical prostatectomy. World J Urol. In press.
[90] Padhani AR, Koh D-M, Collins DJ. Whole-body diffusion-weighted MR imaging in cancer: current status and research directions. Radiology 2011;261:700–18.
[91] Lecouvet FE, El Mouedden J, Collette L, et al. Can whole-body magnetic resonance imaging with diffusion-weighted imaging replace Tc 99m bone scanning and computed tomography for single-step detection of metastases in patients with high-risk prostate cancer? Eur Urol 2012;62:68–75.
[92] Koh D-M, Blackledge M, Padhani AR, et al. Whole-body diffusion-weighted MRI: tips, tricks, and pitfalls. AJR Am J Roentgenol 2012;199:252–62.
[93] Lecouvet FE, Vande Berg BC, Malghem J, Omoumi P, Simoni P. Diffusion-weighted MR imaging: adjunct or alternative to T1-weighted MR imaging for prostate carcinoma bone metastases? Radiology 2009;252:624.
[94] Messiou C, Collins DJ, Giles S, et al. Assessing response in bone metastases in prostate cancer with diffusion weighted MRI. Eur Radiol 2011;21:2169–77.
[95] Padhani AR, van Ree K, Collins DJ, D'Sa S, Makris A. Assessing the relation between bone marrow signal intensity and apparent diffusion coefficient in diffusion-weighted MRI. AJR Am J Roentgenol 2013;200:163–70.
[96] Amlani A, Ghosh-Ray S, van Ree K, et al. Relationships between diffusion weighted signal intensity, ADC and water/fat content of malignant bone marrow [abstract 3447]Presented at: International Society for Magnetic Resonance in Medicine annual meeting; April 20–26, Salt Lake City, UT; 2013.
[97] Blackledge MD, Collins DJ, Tunariu N, et al. Assessment of treatment response by total tumor volume and global apparent diffusion coefficient using diffusion-weighted MRI in patients with metastatic bone disease: a feasibility study. PLoS One 2014;9:e91779.
[98] Hamstra DA, Rehemtulla A, Ross BD. Diffusion magnetic resonance imaging: a biomarker for treatment response in oncology. J Clin Oncol 2007;25:4104–9.
[99] Li SP, Padhani AR. Tumor response assessments with diffusion and perfusion MRI. J Magn Reson Imaging 2012;35:745–63.
[100] Padhani AR, Makris A, Gall P, Collins DJ, Tunariu N, de Bono JS. Therapy monitoring of skeletal metastases with whole-body diffusion MRI. J Magn Reson Imaging 2014;39:1049–78.
[101] Xu GZ, Li CY, Zhao L, He ZY. Comparison of FDG whole-body PET/CT and gadolinium-enhanced whole-body MRI for distant malignancies in patients with malignant tumors: a meta-analysis. Ann Oncol 2013;24:96–101.
[102] Van den Bergh L, Lerut E, Haustermans K, et al. Final analysis of a prospective trial on functional imaging for nodal staging in patients with prostate cancer at high risk for lymph node involvement. Urol Oncol Semin Orig Investig 2015;33, 109 e23- e31.
[103] Fanti S, Minozzi S, Castellucci P, et al. PET/CT with (11)C-choline for evaluation of prostate cancer patients with biochemical recurrence: meta-analysis and critical review of available data. Eur J Nucl Med Mol Imaging 2016;43:55–69.
[104] Hoff BA, Chughtai K, Jeon YH, et al. Multimodality imaging of tumor and bone response in a mouse model of bony metastasis. Transl Oncol 2012;5:415–21.
[105] Rozel S, Galbán CJ, Nicolay K, et al. Synergy between anti-CCL2 and docetaxel as determined by DW-MRI in a metastatic bone cancer model. J Cell Biochem 2009;107:58–64.
[106] Graham TJ, Box G, Tunariu N, et al. Preclinical evaluation of imaging biomarkers for prostate cancer bone metastasis and response to cabozantinib. J Natl Cancer Inst 2014;106:dju033.
[107] Reischauer C, Froehlich JM, Koh DM, et al. Bone metastases from prostate cancer: assessing treatment response by using diffusion-weighted imaging and functional diffusion maps–initial observations. Radiology 2010;257:523–31.
[108] Messiou C, Giles S, Collins DJ, et al. Assessing response of myeloma bone disease with diffusion-weighted MRI. Br J Radiol 2012;85:e1198–203.
[109] Giles SL, Messiou C, Collins DJ, et al. Whole-body diffusion-weighted MR imaging for assessment of treatment response in myeloma. Radiology 2014;271:785–94.
[110] Hayashida Y, Yakushiji T, Awai K, et al. Monitoring therapeutic responses of primary bone tumors by diffusion-weighted image: initial results. Eur Radiol 2006;16:2637–43.
[111] Ballon D, Watts R, Dyke JP, et al. Imaging therapeutic response in human bone marrow using rapid whole-body MRI. Magn Reson Med 2004;52:1234–8.
[112] Lee KC, Bradley DA, Hussain M, et al. A feasibility study evaluating the functional diffusion map as a predictive imaging biomarker for detection of treatment response in a patient with metastatic prostate cancer to the bone. Neoplasia 2007;9:1003–11.
[113] Oka K, Yakushiji T, Sato H, Hirai T, Yamashita Y, Mizuta H. The value of diffusion-weighted imaging for monitoring the chemotherapeutic response of osteosarcoma: a comparison between average apparent diffusion coefficient and minimum apparent diffusion coefficient. Skeletal Radiol 2010;39:141–6.

Please cite this article in press as: Padhani AR, et al. Rationale for Modernising Imaging in Advanced Prostate Cancer. Eur Urol Focus (2016), http://dx.doi.org/10.1016/j.euf.2016.06.018

[114] Horger M, Weisel K, Horger W, Mroue A, Fenchel M, Lichy M. Whole-body diffusion-weighted MRI with apparent diffusion coefficient mapping for early response monitoring in multiple myeloma: preliminary results. AJR Am J Roentgenol 2011;196:W790–5.

[115] Baunin C, Schmidt G, Baumstarck K, et al. Value of diffusion-weighted images in differentiating mid-course responders to chemotherapy for osteosarcoma compared to the histological response: preliminary results. Skeletal Radiol 2012;41:1141–9.

[116] Uhl M, Saueressig U, Koehler G, et al. Evaluation of tumour necrosis during chemotherapy with diffusion-weighted MR imaging: preliminary results in osteosarcomas. Pediatr Radiol 2006;36:1306–11.

[117] Cappabianca S, Capasso R, Urraro F, et al. Assessing response to radiation therapy treatment of bone metastases: short-term followup of radiation therapy treatment of bone metastases with diffusion-weighted magnetic resonance imaging. J Radiother 2014;2014:698127 In: http://dx.doi.org/10.1155/2014/698127

[118] Thoeny HC, Ross BD. Predicting and monitoring cancer treatment response with diffusion-weighted MRI. J Magn Reson Imaging 2010;32:2–16.

[119] Larbi A, Dallaudière B, Pasoglou V, et al. Whole body MRI (WB-MRI) assessment of metastatic spread in prostate cancer: therapeutic perspectives on targeted management of oligometastatic disease. Prostate 2016;76:1024–33.

[120] Schellhammer PF, Chodak G, Whitmore JB, Sims R, Frohlich MW, Kantoff PW. Lower baseline prostate-specific antigen is associated with a greater overall survival benefit from sipuleucel-T in the Immunotherapy for Prostate Adenocarcinoma Treatment (IMPACT) trial. Urology 2013;81:1297–302.

[121] Crawford ED, Stone NN, Yu EY, et al. Challenges and recommendations for early identification of metastatic disease in prostate cancer. Urology 2014;83:664–9.

[122] Rozet F, Roumeguère T, Spahn M, Beyersdorff D, Hammerer P. Non-metastatic castrate-resistant prostate cancer: a call for improved guidance on clinical management. World J Urol. In press.

[123] Pasoglou V, Larbi A, Collette L, et al. One-step TNM staging of high-risk prostate cancer using magnetic resonance imaging (MRI): toward an upfront simplified 'all-in-one' imaging approach? Prostate 2013;74:469–77.

[124] Linton KD, Catto JWF. Whole-body magnetic resonance imaging and prostate cancer metastases: a new gold standard of detection, but does it help us and at what cost? Eur Urol 2012;62:76–7.

[125] Dimopoulos MA, Hillengass J, Usmani S, et al. Role of magnetic resonance imaging in the management of patients with multiple myeloma: a consensus statement. J Clin Oncol 2015;33:657–64.

Please cite this article in press as: Padhani AR, et al. Rationale for Modernising Imaging in Advanced Prostate Cancer. Eur Urol Focus (2016), http://dx.doi.org/10.1016/j.euf.2016.06.018